

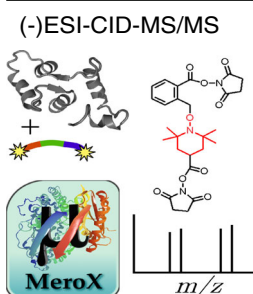
# Dissociation Behavior of a TEMPO-Active Ester Cross-Linker for Peptide Structure Analysis by Free Radical Initiated Peptide Sequencing (FRIPS) in Negative ESI-MS

Christoph Hage,<sup>1</sup> Christian H. Ihling,<sup>1</sup> Michael Götze,<sup>2</sup> Mathias Schäfer,<sup>3</sup> Andrea Sinz<sup>1</sup>

<sup>1</sup>Institute of Pharmacy, Martin Luther University Halle-Wittenberg, Wolfgang-Langenbeck-Str. 4, D-06120, Halle, Saale, Germany

<sup>2</sup>Institute of Biochemistry, Martin Luther University Halle-Wittenberg, Kurt-Mothes-Str. 3, D-06120, Halle, Saale, Germany

<sup>3</sup>Department of Chemistry, University Cologne, Greinstr. 4, D-50939, Köln, Germany



**Abstract.** We have synthesized a homobifunctional amine-reactive cross-linking reagent, containing a TEMPO (2,2,6,6-tetramethylpiperidine-1-oxyl) and a benzyl group (Bz), termed TEMPO-Bz-linker, to derive three-dimensional structural information of proteins. The aim for designing this novel cross-linker was to facilitate the mass spectrometric analysis of cross-linked products by free radical initiated peptide sequencing (FRIPS). In an initial study, we had investigated the fragmentation behavior of TEMPO-Bz-derivatized peptides upon collision activation in (+)-electrospray ionization collision-induced dissociation tandem mass spectrometry (ESI-CID-MS/MS) experiments. In addition to the homolytic NO-C bond cleavage FRIPS pathway delivering the desired odd-electron product ions, an alternative heterolytic NO-C bond

cleavage, resulting in even-electron product ions mechanism was found to be relevant. The latter fragmentation route clearly depends on the protonation of the TEMPO-Bz-moiety itself, which motivated us to conduct (-)-ESI-MS, CID-MS/MS, and MS<sup>3</sup> experiments of TEMPO-Bz-cross-linked peptides to further clarify the fragmentation behavior of TEMPO-Bz-peptide molecular ions. We show that the TEMPO-Bz-linker is highly beneficial for conducting FRIPS in negative ionization mode as the desired homolytic cleavage of the NO-C bond is the major fragmentation pathway. Based on characteristic fragments, the isomeric amino acids leucine and isoleucine could be discriminated. Interestingly, we observed pronounced amino acid side chain losses in cross-linked peptides if the cross-linked peptides contain a high number of acidic amino acids.

**Keywords:** Chemical cross-linking, FRIPS, Negative ESI, Tandem mass spectrometry, TEMPO radical

Received: 9 April 2016/Revised: 14 May 2016/Accepted: 20 May 2016/Published Online: 14 July 2016

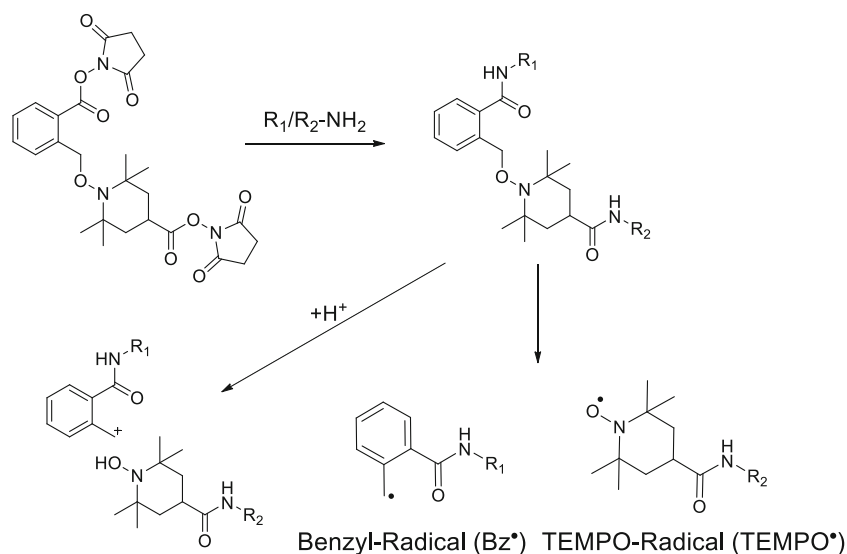
## Introduction

Mass spectrometry (MS) has emerged as a powerful tool for elucidating three-dimensional (3D) structure of proteins and protein complexes [1–5]. As such, chemical cross-linking and footprinting strategies are increasingly employed to derive the topology of proteins and to map interfaces in protein–protein complexes [6]. In chemical cross-linking, the

spatial structure information of a protein or a protein complex is preserved by covalently connecting amino acid side chains. In the majority of cross-linking studies, amine groups of lysines are targeted, but sulfhydryl or carboxylic acid groups might also be addressed by the reactive groups of the cross-linkers [7, 8]. Nonspecific cross-linking via photo-reactive diazirine or benzophenone groups has proven to be beneficial as hydrophobic amino acids are also amenable to the cross-linking reaction [9]. Notably, diazirine photochemistry has shown to be a promising tool for the investigation of peptide–peptide ion interactions in the gas phase when combined with molecular dynamics [10]. The covalent connections created during the cross-linking reaction are either intermolecular (between two different proteins/peptide chains, type 2 cross-link) or intramolecular (within one peptide chain, type 1 cross-link)

**Electronic supplementary material** The online version of this article (doi:10.1007/s13361-016-1426-9) contains supplementary material, which is available to authorized users.

Correspondence to: Mathias Schäfer; e-mail: mathias.schaefer@uni-koeln.de, Andrea Sinz; e-mail: andrea.sinz@pharmazie.uni-halle.de



**Scheme 1.** CID fragmentation of TEMPO-Bz-linker. A mobile proton can result in the protonation of the NO–C bond of the TEMPO-Bz-cross-linker (left hand side). This leads to the formation of a carbocation (i.e., benzylium cation) and a deactivated TEMPO species (i.e., a hydroxylamine). The protonation depends on the positive charge state of the precursor ion and charge localization. Precursor ions that are sodiated or show a strong charge confinement (e.g., arginine-rich amino acid sequences) undergo this fragmentation pathway only to a lower extent or not at all. In contrast, the non-protonated NO–C bond undergoes homolytic dissociation after collision or photolytic activation (middle and right hand side)

(Supplementary Material, Figure S1) [11]. As only amino acid functionalities within the required spatial proximity are connected, as defined by the spacer length of the cross-linker, different cross-linkers with varying spacer lengths might be employed to obtain complementary 3D-structural information of proteins and protein complexes [12]. To allow an enrichment of cross-linked species by affinity chromatography via biotinylation [13] or click chemistry [14, 15], the cross-linkers can be modified accordingly.

Also, isotope labeling [16–18] or a characteristic fragmentation in MS/MS experiments [19–24] might be used to facilitate the identification of cross-linked species. Several collision-induced dissociation (CID)-MS/MS cleavable cross-linkers are currently available, such as DSSO [19], SuDP [21], BAMG [25], the “Edman-linker” [23], the “urea-linker” (BuUrBu) [26], and CBDPS [13]. These cross-linkers constitute an alternative, highly promising strategy for a reliable automated analysis of cross-

**Table 1.** (FRIPS)-Side Chain Losses of Amino Acids

| Amino acid | Side-chain  | Mass Side-chain [u] | Mass difference fragment # [u] | Mass difference fragment * [u] | Other fragments               | Typical neutral losses | Bz <sup>•</sup> -modified fragment # | Bz <sup>•</sup> -modified fragment * |
|------------|---|---------------------|--------------------------------|--------------------------------|-------------------------------|------------------------|--------------------------------------|--------------------------------------|
| G          | H   | 1.0078              | –                              | –                              | –                             | –                      | –                                    | –                                    |
| A          | CH <sub>3</sub>   | 15.0235             | –                              | 1.0078                         | –                             | –                      | –                                    | –                                    |
| S          | CH <sub>2</sub> OH  | 31.0184             | 30.0106                        | –                              | –                             | H <sub>2</sub> O       | –                                    | –                                    |
| P          | –CH <sub>2</sub> CH <sub>2</sub> CH <sub>2</sub> –                                | –                   | –                              | –                              | –                             | –                      | –                                    | –                                    |
| V          | CH(CH <sub>3</sub> ) <sub>2</sub>   | 43.0548             | 42.0470                        | 15.0235                        | –                             | –                      | –                                    | –                                    |
| T          | CH(OH)CH <sub>3</sub>   | 45.0340             | 44.0262                        | 31.0184                        | 15.0265 (CH <sub>3</sub> )    | H <sub>2</sub> O       | –                                    | –                                    |
| C          | CH <sub>2</sub> SH  | 46.9956             | 45.9877                        | 32.9799                        | –                             | H <sub>2</sub> S       | –                                    | –                                    |
| I          | CH(CH <sub>3</sub> )(C <sub>2</sub> H <sub>5</sub> )                              | 57.0704             | 56.0626                        | 29.0391                        | 15.0265 (CH <sub>3</sub> )    | –                      | –                                    | –                                    |
| L          | CH <sub>2</sub> CH(CH <sub>3</sub> ) <sub>2</sub>                                 | 57.0704             | 56.0626                        | 43.0548                        | 15.0265 (CH <sub>3</sub> )    | –                      | –                                    | –                                    |
| N          | CH <sub>2</sub> CONH <sub>2</sub>   | 58.0293             | 57.0215                        | 44.0136                        | –                             | –                      | –                                    | –                                    |
| D          | CH <sub>2</sub> COOH  | 59.0133             | 58.0055                        | –                              | –                             | CO <sub>2</sub>        | –                                    | 176.0472                             |
| Q          | CH <sub>2</sub> CH <sub>2</sub> CONH <sub>2</sub>                                 | 72.0449             | 71.0371                        | 58.0293                        | –                             | –                      | –                                    | –                                    |
| K          | CH <sub>2</sub> CH <sub>2</sub> CH <sub>2</sub> CH <sub>2</sub> NH <sub>2</sub>   | 72.0813             | 71.0735                        | 58.0657                        | –                             | NH <sub>3</sub>        | 189.1154                             | 176.1075                             |
| E          | CH <sub>2</sub> CH <sub>2</sub> COOH  | 73.0290             | 72.0211                        | 59.0133                        | –                             | CO <sub>2</sub>        | –                                    | –                                    |
| M          | CH <sub>2</sub> CH <sub>2</sub> S(CH <sub>3</sub> )                               | 75.0269             | 74.0190                        | 61.0112                        | –                             | –                      | –                                    | –                                    |
| H          | CH <sub>2</sub> (C <sub>3</sub> H <sub>3</sub> N <sub>2</sub> )                   | 81.0453             | 80.0375                        | 67.0296                        | –                             | –                      | –                                    | –                                    |
| F          | CH <sub>2</sub> (C <sub>6</sub> H <sub>5</sub> )                                  | 91.0548             | 90.0470                        | 77.0391                        | –                             | –                      | –                                    | –                                    |
| R          | CH <sub>2</sub> CH <sub>2</sub> CH <sub>2</sub> (CH <sub>4</sub> N <sub>3</sub> ) | 100.0875            | 99.0797                        | 86.0718                        | 43.0296 (NH <sub>2</sub> CNH) | NH <sub>3</sub>        | –                                    | –                                    |
| Y          | CH <sub>2</sub> (C <sub>6</sub> H <sub>4</sub> )(OH)                              | 107.0497            | 106.0419                       | 93.0340                        | –                             | H <sub>2</sub> O       | –                                    | –                                    |
| W          | CH <sub>2</sub> (C <sub>8</sub> H <sub>6</sub> N)                                 | 130.0657            | 129.0579                       | 116.0500                       | –                             | –                      | –                                    | –                                    |

linked products. Applying one or several of these cross-linking principles even allows the application of cross-linking for studying protein interaction networks in whole cell lysates [27–29].

However, the covalent interconnection of tryptic peptides via cross-linking results in large precursor ions ( $m/z > 1500$ ), which resist efficient collision-induced dissociation analysis with increasing number of oscillators. To overcome this limitation, a CID-cleavable cross-linker should preferably exhibit a labile covalent bond, guaranteeing a favored fragmentation over the peptide backbone under collisional activation.

As reported previously, we have synthesized an asymmetric cross-linker combining the benefits of CID-lability with open-shell chemistry, termed TEMPO-Bz-linker (1-[2-(2,5-dioxopyrrolidine-1-yloxy-carbonyl)-benzyloxy]-2,2,6,6-tetramethylpiperidine-4-carboxylic acid 2,5-dioxopyrrolidine-1-yl ester) [30]. (+)-ESI-MS/MS experiments of cross-linked TEMPO-Bz-peptide precursor ions documented the preferred fragmentation of the NO–C bond between the TEMPO and the Bz part of the linker, resulting in stable TEMPO radical-modified and reactive benzoyl-radical-modified peptide product ions. The latter species can undergo radical-driven peptide fragmentation reactions via a variety of radical rearrangements within the peptide backbone and amino acid side chains, termed free radical induced peptide sequencing (FRIPS) [31]. The FRIPS approach induces an ETD/ECD-like fragmentation in peptides, delivering complementary sequence information of peptides. Inspired by the work of Beauchamp and co-workers [31–33], Blanksby et al. [34], and Oh et al. [35, 36] who employed TEMPO-containing labeling reagents that form radicals upon CID, we synthesized a related homo-bifunctional cross-linker [30] (Scheme 1). As described previously, this novel reagent has been successfully applied for cross-linking in a proof-of-principle study with all 20 proteinogenic amino acids and three model peptides [30]. However, an alternative closed shell fragmentation pathway was observed during (+)-ESI-MS/MS experiments of highly charged peptide precursor ions carrying a higher number of charges than basic sites [34, 37–39]. In these highly positively charged precursor ions, the cross-linker was protonated and a heterolytic cleavage of the NO–C bond occurred, resulting in mass-shifted fragment ions.

Consequently, we now investigate the fragmentation behavior of TEMPO-Bz-linker peptide conjugates in (–)-ESI-MS<sup>n</sup> experiments to avoid an influence of this unwanted alternative fragmentation pathway, which increases the complexity of product ion spectra and therefore limits the applicability of the reagent for automated data interpretation. In negative ion mode, the dissociation energy of the NO–C bond is lowered in the presence of local negative charges resulting in a preferred homolytic cleavage [40].

## Experimental

### Materials

All chemicals and solvents were obtained at the highest purity available (Acros Organics, Geel, Belgium, Sigma-Aldrich, Taufkirchen, Germany, Fluka, Steinheim, Germany, Merck,

**Table 2.** Interpeptide Cross-Linked Products and CID Fragment Ions Resulting from Homolytic Cleavage (NO–C Bond)

| R <sup>1</sup>         | R <sup>2</sup>         | Molecular ion species                |                                      |                                      | CID-MS/MS fragment ions                               |  |
|------------------------|------------------------|--------------------------------------|--------------------------------------|--------------------------------------|---|--|
|                        |                        | [M – 2H] <sup>+</sup> 2 <sup>–</sup> | [M – 3H] <sup>+</sup> 3 <sup>–</sup> | [M – 4H] <sup>+</sup> 4 <sup>–</sup> | [R <sup>1</sup> -Bz – xH] <sup>+</sup> x <sup>–</sup> | [R <sup>2</sup> -TEMPO – xH] <sup>+</sup> x <sup>–</sup> |
| TESTDIKR               | EADYLINKER             | 1247.627                             | 831.416                              | 623.310                              | 1064.514 (x = 1)                                      | 1430.740 (x = 1)   |
| EADYLINKER             | TESTDIKR               | 1247.627                             | 831.416                              | 623.310                              | 531.753 (x = 2)                                       | 714.867 (x = 2)  |
| DRVYIHPF               | DRVYIHPF               | 1194.103                             | 795.733 <sup>n.d.</sup>              | 596.548 <sup>n.d.</sup>              | 1365.656 (x = 1)                                      | 1129.598 (x = 1)   |
| RPVKVYPNGAEDESAEAFPLEF | RPVKVYPNGAEDESAEAFPLEF | 2612.760*                            | 1741.504                             | 1305.876 <sup>n.d.</sup>             | 682.325 (x = 2)                                       | 564.295 (x = 2)  |
|                        |                        |                                      |                                      |                                      | 1161.561 (x = 1)                                      | 1226.645 (x = 1)   |
|                        |                        |                                      |                                      |                                      | 2580.218 <sup>n.d.</sup> (x = 1)                      | 2645.302 <sup>n.d.</sup> (x = 1)                         |
|                        |                        |                                      |                                      |                                      | 1289.605 <sup>n.d.</sup> (x = 2)                      | 1322.147 <sup>n.d.</sup> (x = 2)                         |

Singly deprotonated molecular ions [M–H]<sup>–</sup> are not detected as they are outside the mass range analyzed.

\* ... was not detected – out of limit of mass range

n.d. ... not detected

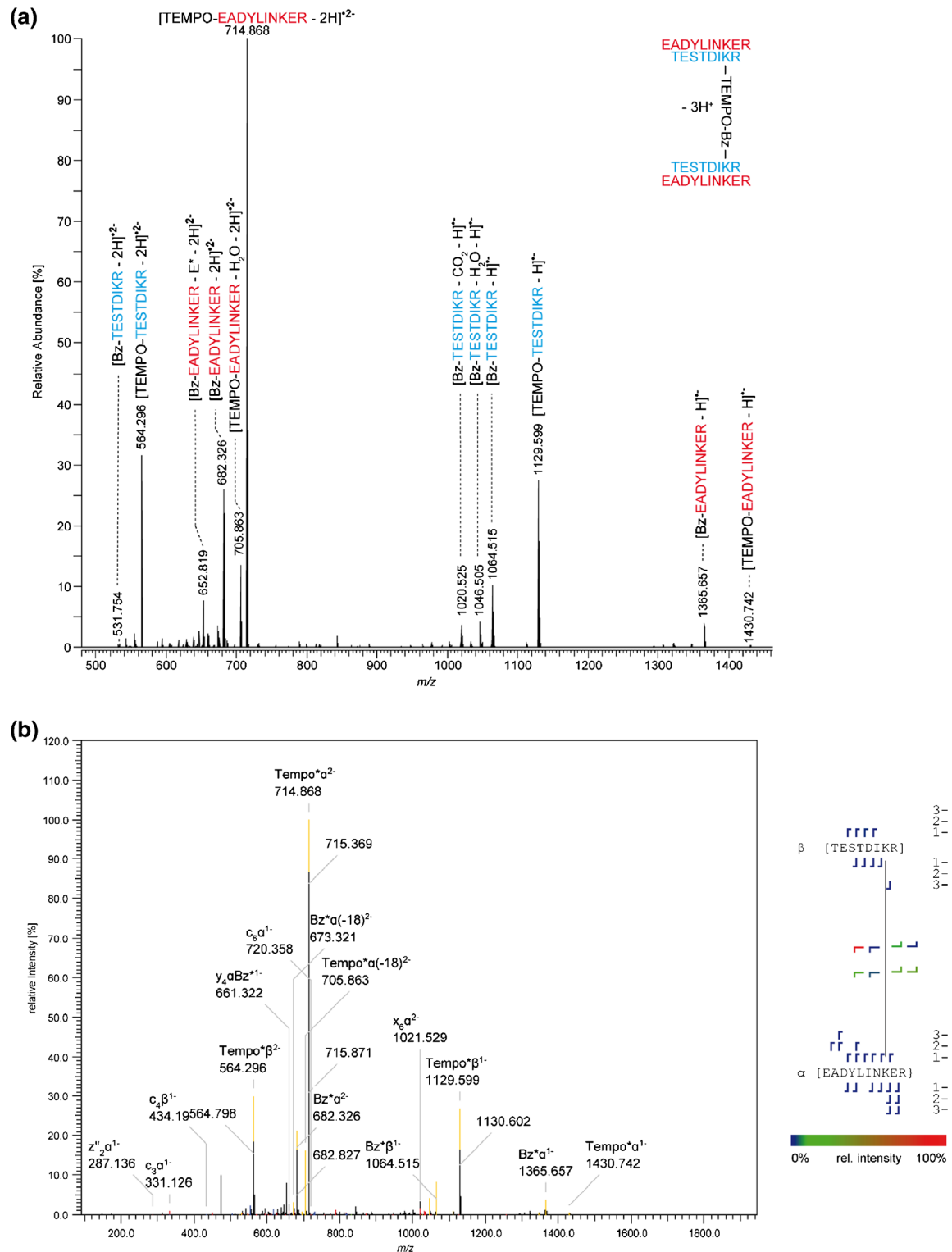


**Figure 1.** (a) (–)-ESI-MS/MS-CID of triply negatively charged TEMPO-Bz-cross-linked tryptic fragments of test peptide 1. Homolytic fragmentation of the TEMPO-Bz-cross-linker mainly leads to the formation of singly and doubly charged TEMPO<sup>•-</sup>- and Bz<sup>•-</sup>-fragments of both peptide chains. In addition, neutral losses of H<sub>2</sub>O and CO<sub>2</sub> are observed as well as side-chain fragmentations of doubly charged Bz<sup>•-</sup>-modified EADYLINKER (i.e., E\* fragment). (b) Automated assignment of fragment ion spectrum by the MeroX software. MeroX assigned most fragment ions to the homolytic cleavage of the TEMPO-Bz-cross-linker or peptide backbone fragmentation. Radical-driven side-chain losses were not defined as neutral losses and were therefore not searched for by MeroX. High sequence coverage was observed by matching low abundant peaks (mainly c-, x-, and z-type ions with different charge states). All assigned peaks were validated manually

Darmstadt, Germany). Human angiotensin II (DRVYIHPF) and human adrenocorticotrophic hormone (ACTH), fragment 18–39 (RPVKVYPNGAEDESAAEAFPLEF) were purchased from Sigma-Aldrich, test peptide 1 (Ac-TRTESTDIKRASSREADYLINKER) was obtained from Creative Molecules Inc. (Victoria BC, Canada). The TEMPO-Bz-linker was synthesized as described previously [30].

### Cross-Linking Experiments

The TEMPO-Bz-linker (1 mM in DMSO) was added to the respective peptide solution (50  $\mu$ M in 20 mM HEPES buffer, pH 8.5) to give a final concentration of 50  $\mu$ M (cross-linker/peptide molar ratio 1:1). The reaction was allowed to proceed for 2 h at room temperature and was quenched by addition of freshly prepared 1 M (NH<sub>4</sub>)HCO<sub>3</sub> solution (final concentration 50 mM). Test peptide 1 was digested with trypsin (Promega, Mannheim, Germany) at 37 °C for 3 h after the cross-linking reaction, whereas angiotensin II and ACTH were not subjected to enzymatic digestion.

### Offline Nano-ESI-Orbitrap-MS

Peptide samples were desalted with C18 ZipTip columns (Millipore); 0.5  $\mu$ L of ammonia solution (30%) were added before conducting (–)-ESI-MS/MS experiments. Samples were measured immediately after sample preparation. Offline nano (+) and (–)-ESI-MS/MS analyses were performed on an Orbitrap Fusion Tribrid mass spectrometer (Thermo Fisher Scientific, San Jose, CA) with nano-ESI source (Nanospray Flex Ion Source; Thermo Fisher Scientific). Samples were loaded into gold-coated

capillaries (4", 1.2 mm/0.68 mm o.d./i.d., World Precision Instruments, Sarasota, FL) that were prepared in-house (Model P-1000 Flaming/Brown Micropipette Puller; Sutter Instruments, Novato, CA). The voltage was set to 1.3 kV in positive ionization mode and to –1.1 to –1.2 kV in negative ionization mode. The source temperature was held at 275 °C. MS data were collected in the *m/z* range 300–1500. For MS/MS measurements, ions were isolated in the quadrupole (isolation window 2 Da), fragmented by CID (20%–35% normalized collision energy; NCE), and fragment ions were analyzed in the Orbitrap mass analyzer (R = 120,000 at *m/z* 200) with external calibration (experimental error < 3 ppm).

### Identification of Cross-Linked Products

MS data were processed with the Proteome Discoverer 1.4 (Thermo Fisher Scientific) creating a list of all precursor ions. The identification of cross-linked peptides was performed with the MeroX 1.5.1 software [41]. Mass tolerance in MeroX data analysis was set to 5 ppm (MS) and 10 ppm (MS/MS and MS<sup>3</sup>).

## Results

### Cross-Linking with Test Peptide 1

Test peptide 1 (Ac-TRTESTDIKRASSREADYLINKER) with acetylated *N*-terminus was chosen as the model peptide for cross-linking as it possesses two lysines at positions 9 and 22 as potential reaction sites of the TEMPO-Bz-linker. Tryptic digestion of the intramolecularly cross-linked peptide delivers the isobaric, reverse-order cross-linked products TESTDIKR-

**Table 3.** Intrapeptide (Type 1) and “Dead-End” (Type 0) Cross-Linked Products

| R <sup>1</sup>          | R <sup>2</sup>              | Molecular ion species |                                      |                                      |                                      |
|-------------------------|-----------------------------|-----------------------|--------------------------------------|--------------------------------------|--------------------------------------|
|                         |                             | [M – H <sup>+</sup> ] | [M – 2H <sup>+</sup> ] <sup>2-</sup> | [M – 3H <sup>+</sup> ] <sup>3-</sup> | [M – 4H <sup>+</sup> ] <sup>4-</sup> |
| TESTDIKR                | (Type I, intra)             |                       |                                      |                                      |                                      |
|                         | -(Bz-TEMPO)-                | 1246.6318             | 622.8123                             | 414.8724 <sup>n.d.</sup>             | 310.9025 <sup>n.d.</sup>             |
|                         | (Type 0, dead-end)          |                       |                                      |                                      |                                      |
| EADYLINKER              | -(Bz-TEMPO)-OH              | 1264.6423             | 631.8175                             | 420.8759                             | 315.4051 <sup>n.d.</sup>             |
|                         | -(Bz-TEMPO)-NH <sub>2</sub> | 1263.6583             | 631.3225                             | 420.5479 <sup>n.d.</sup>             | 315.1591 <sup>n.d.</sup>             |
|                         | (Type I, intra)             |                       |                                      |                                      |                                      |
| DRVYIHPF                | -(Bz-TEMPO)-                | 1547.7744*            | 773.3836                             | 515.2533                             | 386.1881 <sup>n.d.</sup>             |
|                         | (Type 0, dead-end)          |                       |                                      |                                      |                                      |
|                         | -(Bz-TEMPO)-OH              | 1565.7849*            | 782.3888                             | 521.2568                             | 390.6908 <sup>n.d.</sup>             |
| RPVKVYPNGAEDESAAEAFPLEF | -(Bz-TEMPO)-NH <sub>2</sub> | 1564.8009*            | 781.8968                             | 520.9288                             | 390.4448 <sup>n.d.</sup>             |
|                         | (Type I, intra)             |                       |                                      |                                      |                                      |
|                         | -(Bz-TEMPO)-                | 1343.6794             | 671.3361                             | 447.2216 <sup>n.d.</sup>             | 335.1644 <sup>n.d.</sup>             |
| EADYLINKER              | (Type 0, dead-end)          |                       |                                      |                                      |                                      |
|                         | -(Bz-TEMPO)-OH              | 1361.6900             | 680.3413                             | 453.2251                             | 339.6670 <sup>n.d.</sup>             |
|                         | -(Bz-TEMPO)-NH <sub>2</sub> | 1360.7059             | 679.8493                             | 452.8971 <sup>n.d.</sup>             | 339.4210 <sup>n.d.</sup>             |
| TESTDIKR                | (Type I, intra)             |                       |                                      |                                      |                                      |
|                         | -(Bz-TEMPO)-                | 2762.3359*            | 1,380.6643                           | 920.1071                             | 689.8285                             |
|                         | (Type 0, dead-end)          |                       |                                      |                                      |                                      |
| EADYLINKER              | -(Bz-TEMPO)-OH              | 2780.3465*            | 1389.6696                            | 926.1107                             | 694.3312                             |
|                         | -(Bz-TEMPO)-NH <sub>2</sub> | 2779.3625*            | 1389.1776                            | 925.7826 <sup>n.d.</sup>             | 694.0852 <sup>n.d.</sup>             |

\* ... was not detected – out of limit of mass range

n.d. ... not detected

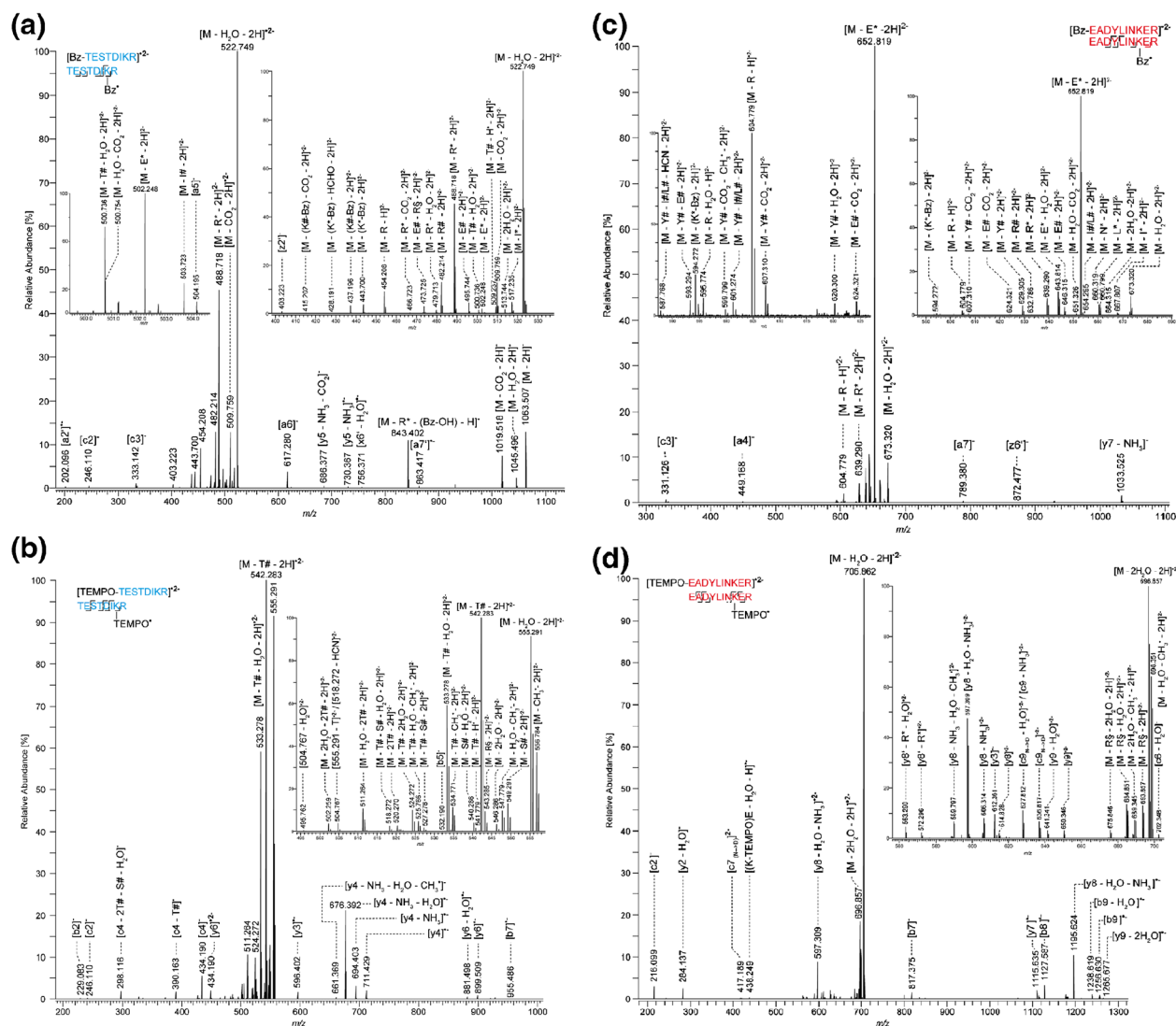
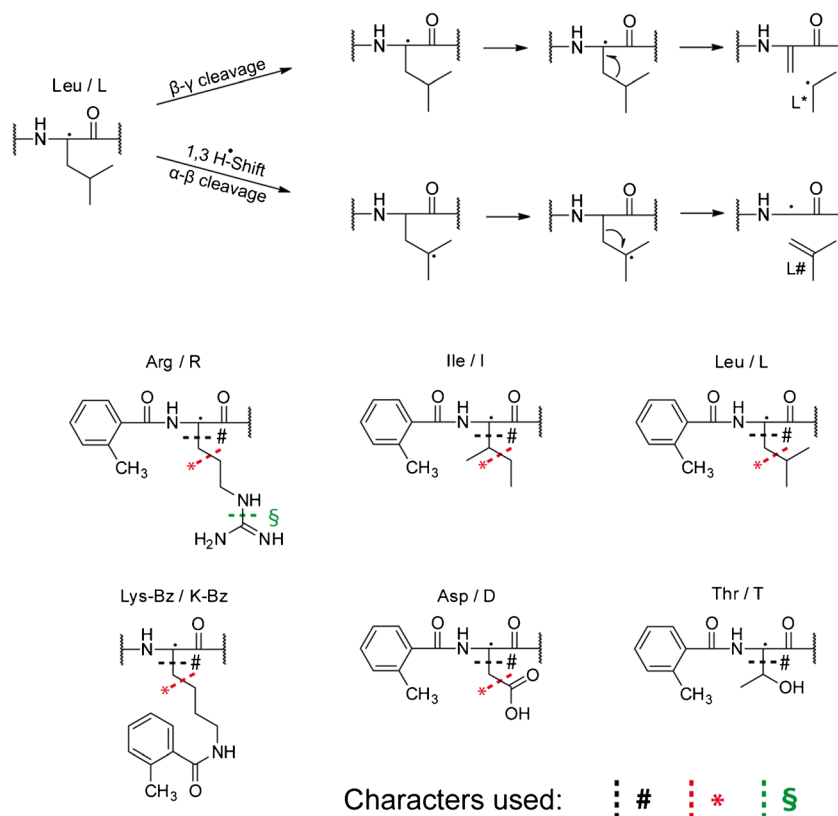


**Figure 2.** (–)-ESI-CID-MS<sup>3</sup> fragment ion spectra of doubly negatively charged Bz<sup>•-</sup> and TEMPO<sup>•-</sup>-modified TESTDIKR and EADYLINKER (NCE 35%). **(a)** The fragment ion spectrum of the doubly negative charged Bz<sup>•-</sup>-TESTDIKR precursor ion ( $m/z$  531.754) shows a region between  $m/z$  400 and 530 that is highly populated by doubly charged fragment ions from side-chain fragmentation and neutral losses. Peptide backbone fragment ions are only observed as singly charged species. Also, a charge-reduced precursor ion is observed at  $m/z$  1063.507. **(b)** The fragment ion spectrum of the doubly negative charged TEMPO<sup>•-</sup>-TESTDIKR precursor ion ( $m/z$  564.296) shows a region between  $m/z$  490 and 560 that is highly populated by doubly charged fragment ion peaks derived from side-chain fragmentation and neutral losses. Peptide backbone fragment ions are only observed as singly charged species. The only exception is the  $y_6$  ion, which is observed as singly and doubly charged species. Interestingly, the spectrum is dominated by backbone fragmentation near the acidic amino acids (i.e., Glu-2 and Asp-5 leading to  $y_3$ ,  $y_4$ , and  $y_6$  as well as  $b_2$ ,  $b_4$ ,  $c_4$ ,  $b_5$  ions). Also a low-intense peak is observed for the  $b_7$  ion, derived from the loss of the C-terminal arginine. As shown in the inset, several side-chain losses can occur. Only losses of the AA#-type can occur multiple times, due to the remaining radical character of the precursor ion. **(c)** The fragment ion spectrum of the doubly negative charged Bz<sup>•-</sup>-EADYLINKER- precursor ion ( $m/z$  682.326) shows a region between  $m/z$  580 and 680 that is highly populated by doubly charged fragment ion peaks derived from side chain fragmentation and neutral losses. Remarkably, the radical driven side-chain loss of E<sup>\*</sup> is dominant for this peptide sequence and forms the base peak. Also side chain losses of E, R, and Y dominate the spectra. Peptide backbone fragment ions are only observed as singly charged species and are mainly centered on the Tyr-4. Except for the  $y_7$  ion, only a-, c-, and z-type ions were observed (i.e.,  $c_3$ ,  $a_4$ ,  $z_6'$ ,  $a_7$ ). Leucine and isoleucine could be discriminated by the loss of L<sup>\*</sup> ( $m/z$  660.799) or I<sup>\*</sup> ( $m/z$  667.807), respectively. **(d)** The fragment ion spectrum of the doubly negative charged TEMPO<sup>•-</sup>-TESTDIKR precursor ion ( $m/z$  714.868) shows a region between  $m/z$  670 and 700 that is populated mainly by doubly charged fragment ions derived from side chain fragmentations of arginine and neutral losses. A second region between  $m/z$  560 and 650 shows mainly doubly charged  $y_8$ ,  $y_9$ , and  $c_9$  fragment ion peaks with additional neutral losses and arginine side chain losses. Especially  $c_9$ - and  $c_7$ -fragments yield evidence for a partly deamidation of glutamine. Peptide backbone fragmentation occurs mainly proximal to the three acidic amino acids (i.e., Glu-1, Asp-3, Glu-9) and the (partly deamidated) glutamine (Gln-7)

Tempo-Bz-EADYLINKER and EADYLINKER-TEMPO-Bz-TESTDIKR (Tables 1 and 2), in which the two lysines (Lys-9 and Lys-22) are connected via the cross-linker. The (-)-ESI mass spectrum documents the formation of the doubly ( $m/z$  1247.127), triply ( $m/z$  831.750), and quadruply ( $m/z$  623.312) deprotonated molecular ions  $[M - nH]^{n-}$  of the cross-linked peptide as well as crosslinker-modified TESTDIKR and EADYLINKER peptide fragments (doubly charged species, Supplementary Material, Figure S2) and the unmodified EADYLINK peptide fragment (singly and doubly charged species). The (-)-ESI-CID fragment ion spectrum of the doubly deprotonated precursor ion exhibited both singly charged radical product ions (Bz $\cdot$ - and TEMPO $\cdot$ -modified) of TESTDIKR ( $m/z$  1064.514 and 1129.598) and EADYLINKER ( $m/z$  1365.656 and 1430.740) fragments (Table 2). The (-)-ESI-CID product ion spectrum of the triply charged precursor ion ( $m/z$  831.416) also showed doubly charged open-shell product ions of TESTDIKR ( $m/z$  531.753 and 564.295) and EADYLINKER ( $m/z$  682.325 and 714.867) (Figure 1a and Table 2). Furthermore, neutral losses of CO<sub>2</sub>, H<sub>2</sub>O, as well as a prominent side chain loss of glutamic acid

residues from the Bz-radical-modified EADYLINKER peptide were observed. An automated assignment of the FRIPS product ion signals by MeroX delivered high sequence coverage via backbone fragmentation of the cross-linked peptide, namely c-, x-, and z-type ions (Figure 1b). To investigate the fragmentation behavior of negatively charged Bz $\cdot$ - and TEMPO $\cdot$ -modified peptide ions, doubly deprotonated precursor ions were selected for CID-MS<sup>3</sup> experiments. The fragmentation of the Bz-radical-modified TESTDIKR peptide ion (Figure 2a) resulted mainly in side chain losses of amino acids (for nomenclature please refer to Scheme 2), which is in good agreement with the proposed FRIPS mechanism. Moreover, a number of peptide backbone fragments were observed. In contrast, the TEMPO $\cdot$ -modified TESTDIKR peptide ion (Figure 2b) exhibited less side chain fragments, mainly originating from hydroxylic amino acids, but a rich peptide backbone fragmentation. Accordingly, CID-MS<sup>3</sup> experiments of the doubly charged Bz $\cdot$ -modified EADYLINKER peptide fragment (Figure 2c) preferably showed side chain losses (for nomenclature please refer to Scheme 2) as well as a few backbone cleavages.



**Scheme 2.** Nomenclature of radical driven side-chain fragmentation used in this paper. After radical transfer to the  $\alpha$ -carbon of a peptide chain by hydrogen rearrangement, different fragmentation pathways are observed. If the bond between  $\alpha$ - and  $\beta$ -carbon of the amino acid is cleaved, the radical remains at the peptide chain, resulting in the loss of an alkene (indicated as #). An alternative 1,3-hydrogen shift leads to a  $\gamma$ -carbon radical. If the bond between  $\beta$ - and  $\gamma$ -carbon is cleaved, the alkene remains at the precursor ion, resulting in the loss of one carbon shortened side-chain radical (indicated as \*). For arginine-containing species, the loss of a carbodiimide-like species is observed (indicated as §). It has to be pointed out that for some amino acids (e.g., glycine, proline) not all pathways are possible

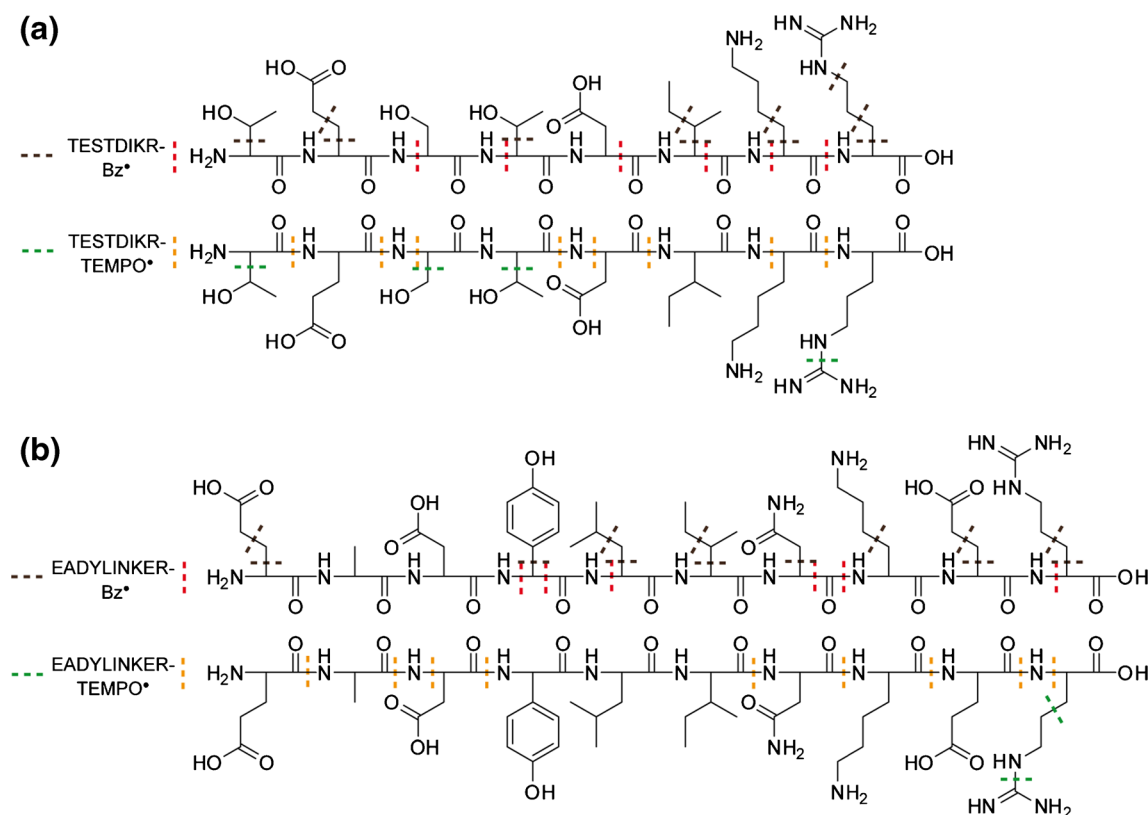
Intriguingly, the characteristic fragments even allowed discriminating the isobaric amino acids leucine and isoleucine (Scheme 3). On the other hand, the doubly charged TEMPO<sup>•</sup>-modified EADYLINKER peptide ion (Figure 2d) delivered a limited number of side chain fragments in addition to a wealth of backbone fragments. An overview of the complementary fragmentation behavior of Bz<sup>•</sup>- and TEMPO<sup>•</sup>-modified peptide fragments is depicted in Scheme 3 for TESTDIKR (a) and EADYLINKER (b).

### Cross-Linking with Angiotensin II

Additionally, we analyzed angiotensin II (DRVYIHPF) in our (–)-ESI-CID-MS/MS experiments as this peptide had already been used as a model compound for a TEMPO-Bz-labeling reagent in a previous (+)-ESI-MS/MS study conducted by Lee et al. [36]. Angiotensin II possesses an *N*-terminal amine group (Asp-1) and a phenolic hydroxyl functionality (Tyr-4) for NHS-mediated cross-linking [42]. Non-reacted peptide, “dead-end” (type 0), and intramolecular (type 1) cross-links dominated the TEMPO-Bz-cross-linked angiotensin II experiments (Table 3). “Dead-end” cross-linked product ion species were

subjected to CID-MS/MS for comparison with the reported data set of TEMPO-Bz-labeled angiotensin II in (+)-ESI-MS/MS (*m/z* 1361.690, hydrolyzed species) and (–)-ESI-MS/MS (*m/z* 1360.706, amidated species) experiments (Supplementary Material, Table S1). On the other hand, the products of interpeptide (type 2) cross-linking (*m/z* 1194.103) were exclusively subjected to CID-ESI-MS/MS in the negative ionization mode (Figure 3). The (–)-ESI-CID product ion mass spectrum of amidated TEMPO-Bz-modified angiotensin II (type 0 cross-link, doubly charged species) documented the homolytic cleavage of the NO-C bond of the cross-linker. An abundant signal of intact TEMPO<sup>•</sup>- together with a less abundant one of a Bz<sup>•</sup>-modified peptide as well as water losses from the precursor ion and the homolytic cleavage products were observed (data not shown). Additionally, the Bz<sup>•</sup>-modified species showed the loss of CO<sub>2</sub>. FRIPS-like *x*- and *z*-type fragment ions of the peptide backbone as well as Bz<sup>•</sup>-modified *a*-type products were observed in addition to a *y*<sub>7</sub> fragment ion (fragmentation of the peptide bond between Asp-1 and Arg-2; Supplementary Material, Table S1).

In contrast, the product ion mass spectrum of the interpeptide (type 2) cross-linked angiotensin species



**Scheme 3.** Fragmentations observed for TEMPO-Bz-cross-linked and tryptically digested test peptide 1; (a) TESTDIKR and (b) EADYLINKER. Complementary structural information is obtained by (–)-ESI-CID-MS<sup>3</sup> for tryptic fragments of test peptide 1. Side-chain fragmentation are visualized as black (Bz<sup>•</sup>-modified) and green (TEMPO<sup>•</sup>-modified) dashed lines. Backbone fragmentation is visualized in red (Bz<sup>•</sup>-modified) and yellow (TEMPO<sup>•</sup>-modified). A highly complementary fragmentation behavior is observed for different modifications. Losses of neutrals (i.e., H<sub>2</sub>O, NH<sub>3</sub>, CO<sub>2</sub>) or ambiguous losses (i.e., CH<sub>3</sub>- radical) are not indicated



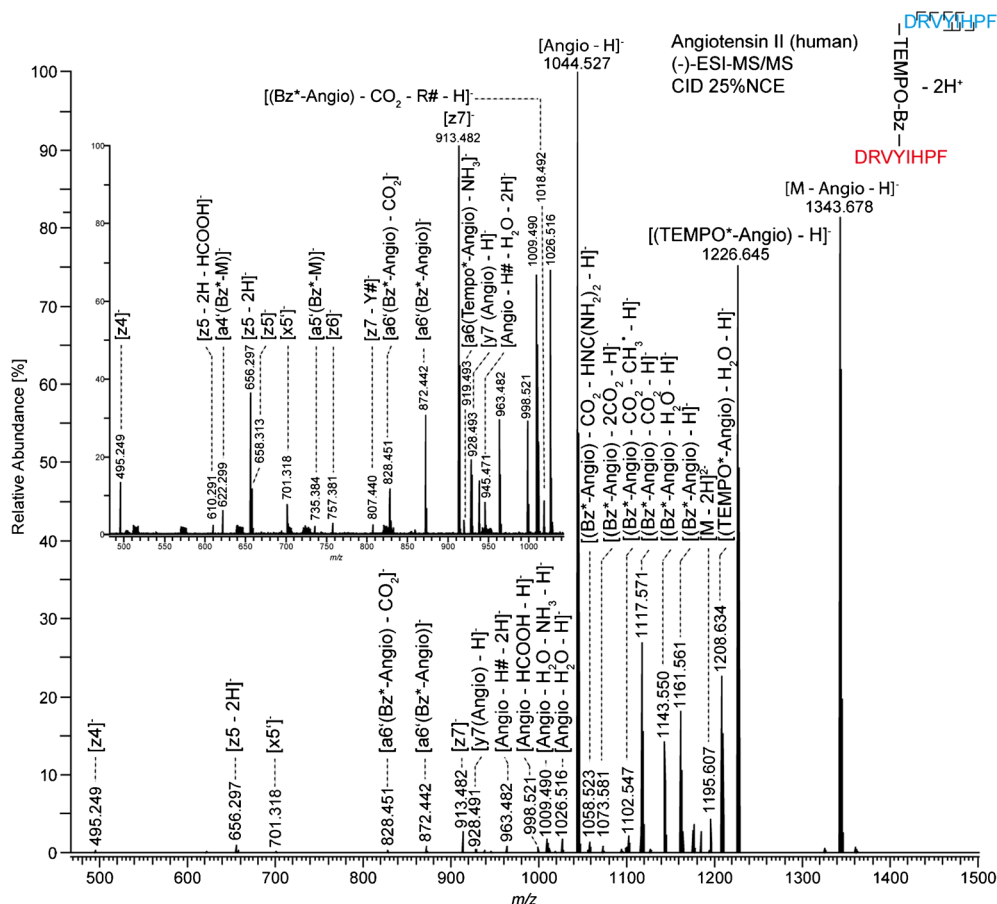


**Figure 3.** (-)-ESI-CID fragment ion mass spectrum of doubly deprotonated, interpeptide TEMPO-Bz-cross-linked angiotensin II (precursor  $m/z$  1194.103)

showed mainly two abundant fragment ion signals as Figure 3 illustrates. Remarkably, a signal of the deprotonated intact angiotensin peptide ( $m/z$  1044.528) and a species isobaric to an intra-peptide (type 1) cross-link at  $m/z$  1343.679 are found. Peptide backbone fragment ions (x- and z-type ions) were low abundant and b-type ions were not detected at all. Furthermore, side chain fragments of histidine and arginine residues were observed. Mainly Bz<sup>•</sup>-modified a-type fragment ions were found with moderate intensities and allowed obtaining sequence coverage of angiotensin II comparable to the previously conducted FRIPS studies [36].

### Cross-Linking with ACTH

ACTH (RPVKVYPNGAEDESAEAFPLEF) was used as the model peptide with a low pI of  $\sim 4.25$ , containing five acidic amino acids (one aspartic acid, four glutamic acid residues). It exhibits an *N*-terminal arginine and a lysine at position 4, both suitable for NHS-mediated cross-linking. Therefore, at least four protons are available for dissociation resulting in a net charge of  $-4$  per peptide molecule, which would allow the investigation of highly charged interpeptide (type 2) cross-linked species.

Also, ACTH does not exhibit an acidic *N*-terminal residue as in angiotensin II. Therefore, ACTH will serve as a suitable model to investigate the special importance of this residue for the peculiar cleavage of one complete peptide in type 2 cross-links. Surprisingly, mainly unmodified peptides dominated the (-)-ESI mass spectrum after the cross-linking reaction with ACTH ( $[M - 2H]^{2-}$  at  $m/z$  1231.590 and  $[M - 3H]^{3-}$  at  $m/z$  820.725) (data not shown). The interpeptide (type 2) cross-linked product was exclusively detected as triply charged species ( $m/z$  1741.838), whereas “dead-end” (type 0) cross-linked products were observed as doubly ( $m/z$  1390.171) and triply ( $m/z$  926.779) charged species. The corresponding intrapeptide (type 1) cross-links ( $m/z$  1381.165 and 920.442) were also found with high abundance.

The (-)-ESI-CID fragment ion spectrum of the triply charged, interpeptide cross-linked species revealed an even more dominant fragmentation pathway via loss of a complete peptide chain as Figure 4 documents. Neither backbone fragmentation nor side chain fragmentations were observed. In contrast, singly ( $m/z$  2465.866) and doubly ( $m/z$  1232.425) charged ACTH peptide species were observed in addition to the corresponding fragment ions of TEMPO-Bz-linker-modified peptide (singly

charged species at  $m/z$  2765.223, doubly charged species at  $m/z$  1382.104). The CID process of the triply charged, interpeptide cross-linked ion species at  $m/z$  1741.838 delivered a prevailing charge separation between the two product ions in MS/MS experiments. Usually, the expelled ACTH peptide carries only one charge, while the remaining cross-linker-modified peptide accommodates the residual two charges of the precursor ion.

## Discussion

The (-)-ESI-MS<sup>n</sup> experiments of TEMPO-Bz-modified peptides delivered highly promising results and emphasize the beneficial features of the reagent for crosslinking studies. Negative ion mode MS/MS of cross-linked test peptide 1 showed a fragmentation behavior similar to that in positive ion mode [30]. For all observed charge states, the desired homolytic cleavage of the NO-C bond of TEMPO-Bz-linker was observed and abundant open shell product ions were generated. Subsequent CID-MS<sup>3</sup> experiments of the open-shell fragment ions (i.e., Bz<sup>•</sup>-peptide and TEMPO<sup>•</sup>-peptide species), confirmed the differences in reactivity of the two peptide radicals. Various complementary backbone (MS<sup>3</sup> of peptide-TEMPO<sup>•</sup>

fragment) and side chain fragmentations (MS<sup>3</sup> of peptide-Bz<sup>•</sup> fragment, also found in MS/MS) permitted nearly complete sequence coverage and allowed discrimination between the isomeric amino acids leucine and isoleucine (Figure 2c, Scheme 3b). The fragmentation behavior of TEMPO-Bz-labeled angiotensin II [36] in (+)- and (-)-ESI-MS<sup>n</sup> is in full agreement with earlier reports on characteristic peptide fragmentation patterns resulting from FRIPS (Supplementary Material, Table S1). In conclusion, the FRIPS chemistry originally designed for TEMPO-Bz-labeled peptides is preserved for cross-linked peptides and is predictable and effective for the FRIPS-driven analysis of cross-linked peptides in (-)-ESI-MS/MS. The closed-shell fragmentation pathway found for multiply protonated TEMPO-Bz-peptide precursor ions in (+)-ESI-MS/MS that limits the applicability of this reagent was completely absent in (-)-ESI-MS/MS, supporting our assumption that a heterolytic cleavage of the NO-C bond depends on the initial protonation of the TEMPO-Bz-linker itself [43]. Therefore, the TEMPO-Bz-linker allows a rapid and unambiguous identification of cross-linked species via the homolytic linker fragmentation in a (-)-ESI-MS/MS workflow, creating a “doublet” for each cross-linked peptide. Strikingly, an unexpected cleavage reaction

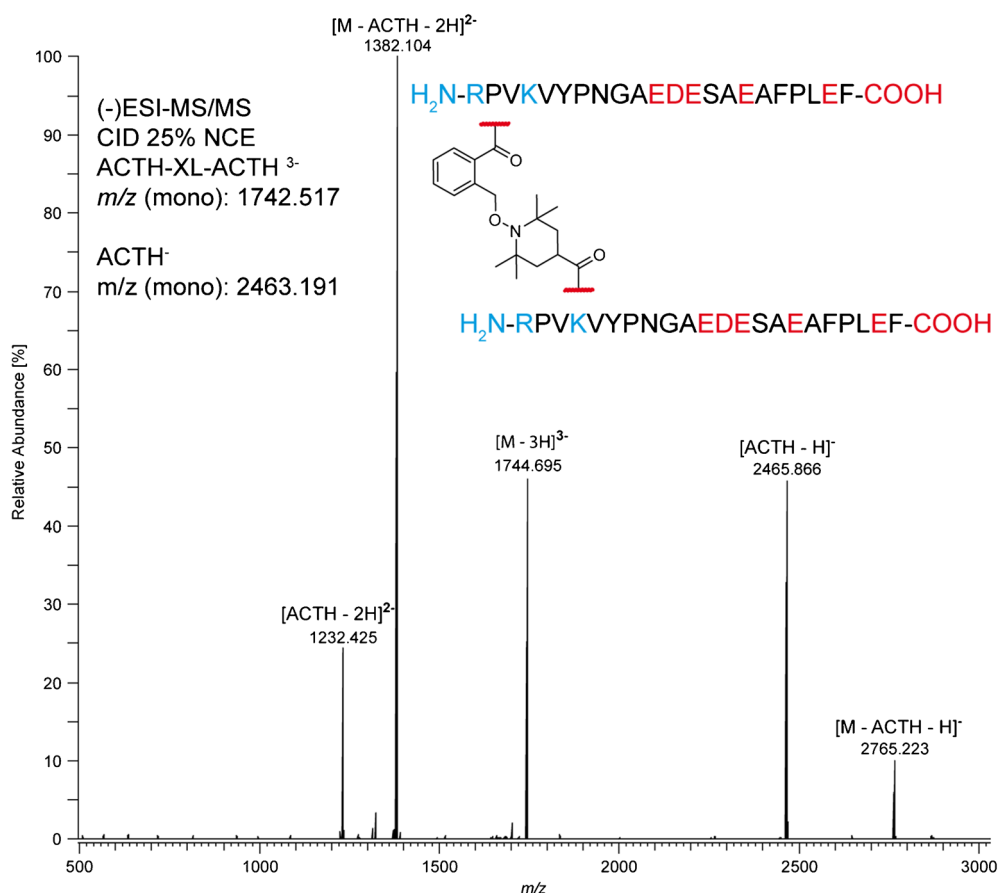
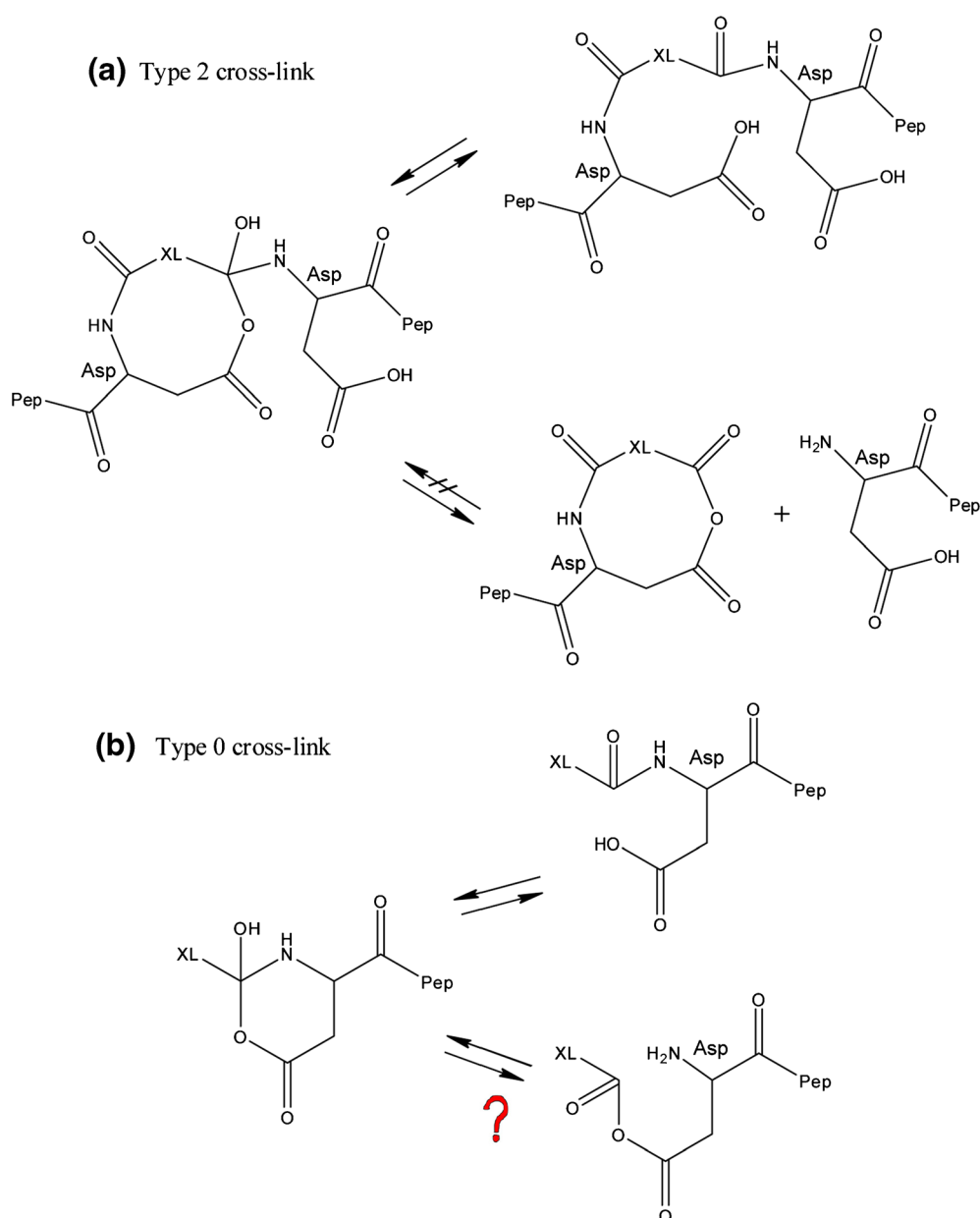


**Figure 4.** (-)-ESI-CID fragment ion mass spectrum of doubly deprotonated, interpeptide TEMPO-Bz cross-linked ACTH (precursor  $m/z$  1742.170)

leading to the loss of an entire peptide chain was observed in (-)-ESI-MS/MS for interpeptide (type 2) cross-linked precursor ions containing acidic amino acids. This pathway was the dominant fragmentation pathway for interpeptide cross-links of angiotensin II and ACTH (Figures 3 and 4), but was not observed for “dead-end” (type 0) cross-links [36]. The results point towards the involvement of carboxylic acid side chain residues at certain positions in the peptides studied herein as shown in Scheme 4. In angiotensin II, only the *N*-terminal amine group is available for NHS-mediated cross-linking. A rearrangement of the *N*-terminal Asp’s carboxylic side chain towards the cross-linker amide bond is conceivable [44], but experimental findings suggest that the presence

of more than one acidic amino acid side chain is essential. In an interpeptide cross-link, the carboxylic side chain of the first peptide might attack the amide bond between the cross-linker and the second peptide chain as shown in Scheme 4. This nucleophilic attack leads to the release of the complete peptide chain attached to the cross-linker, resulting in an intact and unmodified peptide ion and a fragment ion isobaric to an intrapeptide (type 1) cross-link. The formation of these two specific product ions is not possible for “dead-end” (type 0) cross-links (Scheme 4). Interestingly, already the limited number of examples of this initial data set suggests that the fragmentation mechanisms and prerequisites for the appearance of these characteristic fragments are more



**Scheme 4.** (a) Postulated mechanism for the peptide loss observed for interpeptide (type 2) cross-links. (b) A comparable mechanism of an intramolecular rearrangement would not be distinguishable for “dead-end” (type 0) cross-links

complicated. First, the loss of a complete peptide chain is not limited to peptides containing an acidic *N*-terminal amino acid as the results with ACTH suggest. For intermolecularly cross-linked ACTH, containing an *N*-terminal highly basic arginine residue, the loss of a peptide chain was the only observed fragmentation pathway (Figure 4). Besides the *N*-terminus (Arg-1), three reaction sites for the TEMPO-Bz-linker are available in ACTH: (1) The presumably most reactive amine group is Lys-4, with no acidic amino acid in close proximity; (2) the less reactive hydroxyl group of Ser-14 resides adjacent to Glu-13, being close to Glu-11, Asp-12, and Glu-16; and finally, (3) the phenolic hydroxyl group of Tyr-6 is also not adjacent to an acidic amino acid residue. In any case, the release of an intact ACTH peptide molecule necessitates the intramolecular nucleophilic attack of an acidic amino acid residue towards the amide bond between cross-linker and peptide. Second, analysis of cross-linked peptides originating from test peptide 1 (TESTDIKR and EADYLINKER) containing five acidic amino acids does not show the loss of an entire peptide. The EADYLINKER fragment exhibits even a glutamic acid adjacent to the cross-linked lysine.

## Conclusions

Three TEMPO-Bz-peptide model compounds were investigated in (–)-ESI-CID-MS/MS and MS<sup>3</sup> experiments. Non-desired heterolytic cleavage of the TEMPO-Bz-linker that had been observed in (+)-ESI-CID-MS/MS experiments was completely absent in negative ion mode, confirming the previously predicted dependence of this sidetracking fragmentation pathway on the protonation of the TEMPO-Bz-group itself. Only the desired homolytic cleavage of the TEMPO-Bz-linker was observed in (–)-ESI-MS/MS experiments upon CID of cross-linked TEMPO-Bz-peptide ions. The resulting complementary TEMPO<sup>•</sup>- and Bz<sup>•</sup>-radical peptide ions trigger FRIPS, peptide backbone fragmentation, and amino acid side-chain losses and, hence, deliver a broad variety of information leading to exhaustive and reliable structure analysis.

Unexpectedly, an additional fragmentation pathway was found to be relevant for the acidic peptides studied herein, in which one intact peptide chain is completely expelled. To the best of our knowledge, this pathway has not been described before for interpeptide (type 2) cross-linked peptides. Details of the fragmentation reaction mechanism and in particular the influence of acidic amino acid residues at certain positions within the amino acid sequence are by far not completely understood and will be further investigated.

## Acknowledgments

This work is funded by the DFG (projects Si 867/15-2 to A.S. and SCHA 871/7-2 to M.S.) and the region of Saxony-Anhalt.

M.G. is funded by the DFG (FOR855 “Cytoplasmic regulation of gene expression” and GRK1591 “Post-transcriptional control of gene expression—mechanisms and role in pathogenesis”). The authors thank Dr. Francesco Falvo for synthesizing the TEMPO-Bz-linker.

## References

- Rappsilber, J.: The beginning of a beautiful friendship: cross-linking/mass spectrometry and modelling of proteins and multi-protein complexes. *J. Struct. Biol.* **173**, 530–540 (2011)
- Leitner, A., Faini, M., Stengel, F., Aebersold, R.: Crosslinking and mass spectrometry: an integrated technology to understand the structure and function of molecular machines. *Trends Biochem. Sci.* **41**, 20–32 (2016)
- Politis, A., Stengel, F., Hall, Z., Hernandez, H., Leitner, A., Walzthoeni, T., Robinson, C.V., Aebersold, R.: A mass spectrometry-based hybrid method for structural modeling of protein complexes. *Nat. Methods* **11**, 403–406 (2014)
- Walzthoeni, T., Leitner, A., Stengel, F., Aebersold, R.: Mass spectrometry supported determination of protein complex structure. *Curr. Opin. Struct. Biol.* **23**, 252–260 (2013)
- Sinz, A., Arlt, C., Chorev, D., Sharon, M.: Chemical cross-linking and native mass spectrometry: a fruitful combination for structural biology. *Protein Sci.* **24**, 1193–1209 (2015)
- Konermann, L., Vahidi, S., Sowole, M.A.: Mass spectrometry methods for studying structure and dynamics of biological macromolecules. *Anal. Chem.* **86**, 213–232 (2014)
- Petrotchenko, E.V., Borchers, C.H.: Crosslinking combined with mass spectrometry for structural proteomics. *Mass Spectrom. Rev.* **29**, 862–876 (2010)
- Leitner, A., Joachimiak, L.A., Unverdorben, P., Walzthoeni, T., Frydman, J., Forster, F., Aebersold, R.: Chemical cross-linking/mass spectrometry targeting acidic residues in proteins and protein complexes. *Proc. Natl. Acad. Sci. U. S. A.* **111**, 9455–9460 (2014)
- Sinz, A.: The advancement of chemical cross-linking and mass spectrometry for structural proteomics: from single proteins to protein interaction networks. *Expert. Rev. Proteomics* **11**, 733–743 (2014)
- Shaffer, C.J., Andrikopoulos, P.C., Rezac, J., Rulisek, L., Turecek, F.: Efficient covalent bond formation in gas-phase peptide–peptide ion complexes with the photoleucine stapler. *J. Am. Soc. Mass Spectrom.* **27**, 633–645 (2016)
- Schilling, B., Row, R.H., Gibson, B.W., Guo, X., Young, M.M.: MS2Assign, automated assignment and nomenclature of tandem mass spectra of chemically crosslinked peptides. *J. Am. Soc. Mass Spectrom.* **14**, 834–850 (2003)
- Hofmann, T., Fischer, A.W., Meiler, J., Kalkhof, S.: Protein structure prediction guided by crosslinking restraints—a systematic evaluation of the impact of the crosslinking spacer length. *Methods* **89**, 79–90 (2015)
- Petrotchenko, E.V., Serpa, J.J., Borchers, C.H.: An isotopically coded CID-cleavable biotinylated cross-linker for structural proteomics. *Mol. Cell. Proteomics* **10**, 1–8 (2011)
- Chowdhury, S.M., Du, X.X., Tolic, N., Wu, S., Moore, R.J., Mayer, M.U., Smith, R.D., Adkins, J.N.: Identification of cross-linked peptides after click-based enrichment using sequential collision-induced dissociation and electron transfer dissociation tandem mass spectrometry. *Anal. Chem.* **81**, 5524–5532 (2009)
- Burke, A.M., Kandur, W., Novitsky, E.J., Kaake, R.M., Yu, C., Kao, A., Vellucci, D., Huang, L., Rychnovsky, S.D.: Synthesis of two new enrichable and MS-cleavable cross-linkers to define protein–protein interactions by mass spectrometry. *Org. Biomol. Chem.* **13**, 5030–5037 (2015)
- Brodie, N.I., Makepeace, K.A., Petrotchenko, E.V., Borchers, C.H.: Isotopically-coded short-range hetero-bifunctional photo-reactive crosslinkers for studying protein structure. *J. Proteome* **118**, 12–20 (2015)
- Petrotchenko, E.V., Serpa, J.J., Makepeace, K.A., Brodie, N.I., Borchers, C.H.: (14)N(15)N DXMSMS match program for the automated analysis of LC/ESI-MS/MS crosslinking data from experiments using (15)N metabolically labeled proteins. *J. Proteome* **109**, 104–110 (2014)

18. Ihling, C., Schmidt, A., Kalkhof, S., Schulz, D.M., Stingl, C., Mechtler, K., Haack, M., Beck-Sickinger, A.G., Cooper, D.M., Sinz, A.: Isotope-labeled cross-linkers and Fourier transform ion cyclotron resonance mass spectrometry for structural analysis of a protein/peptide complex. *J. Am. Soc. Mass Spectrom.* **17**, 1100–1113 (2006)
19. Kao, A.H., Chiu, C.L., Vellucci, D., Yang, Y.Y., Patel, V.R., Guan, S.H., Randall, A., Baldi, P., Rychnovsky, S.D., Huang, L.: Development of a novel cross-linking strategy for fast and accurate identification of cross-linked peptides of protein complexes. *Mol. Cell. Proteomics* **10**, 1–17 (2011)
20. Soderblom, E.J., Bobay, B.G., Cavanagh, J., Goshe, M.B.: Tandem mass spectrometry acquisition approaches to enhance identification of protein–protein interactions using low-energy collision-induced dissociative chemical crosslinking reagents. *Rapid Commun. Mass Spectrom.* **21**, 3395–3408 (2007)
21. Soderblom, E.J., Goshe, M.B.: Collision-induced dissociative chemical cross-linking reagents and methodology: applications to protein structural characterization using tandem mass spectrometry analysis. *Anal. Chem.* **78**, 8059–8068 (2006)
22. Müller, M.Q., Dreiocker, F., Ihling, C.H., Schäfer, M., Sinz, A.: Fragmentation behavior of a thiourea-based reagent for protein structure analysis by collision-induced dissociative chemical cross-linking. *J. Mass Spectrom.* **45**, 880–891 (2010)
23. Dreiocker, F., Müller, M.Q., Sinz, A., Schäfer, M.: Collision-induced dissociative chemical cross-linking reagent for protein structure characterization: applied Edman chemistry in the gas phase. *J. Mass Spectrom.* **45**, 178–189 (2010)
24. Müller, M.Q., Zeiser, J.J., Dreiocker, F., Pich, A., Schäfer, M., Sinz, A.: A universal matrix-assisted laser desorption/ionization cleavable cross-linker for protein structure analysis. *Rapid Commun. Mass Spectrom.* **25**, 155–161 (2011)
25. Buncherd, H., Roseboom, W., de Koning, L.J., de Koster, C.G., de Jong, L.: A gas phase cleavage reaction of cross-linked peptides for protein complex topology studies by peptide fragment fingerprinting from large sequence database. *J. Proteome* **108**, 65–77 (2014)
26. Müller, M.Q., Dreiocker, F., Ihling, C.H., Schäfer, M., Sinz, A.: Cleavable cross-linker for protein structure analysis: reliable identification of cross-linking products by tandem MS. *Anal. Chem.* **82**, 6958–6968 (2010)
27. Kaake, R.M., Wang, X., Burke, A., Yu, C., Kandur, W., Yang, Y., Novitsky, E.J., Second, T., Duan, J., Kao, A., Guan, S., Vellucci, D., Rychnovsky, S.D., Huang, L.: A new in vivo cross-linking mass spectrometry platform to define protein–protein interactions in living cells. *Mol Cell Proteomics* **13**, 3533–3543 (2014)
28. Liu, F., Rijkers, D.T.S., Post, H., Heck, A.J.R.: Proteome-wide profiling of protein assemblies by cross-linking mass spectrometry. *Nat. Methods* **12**, 1–9 (2015)
29. Chavez, J.D., Schweppe, D.K., Eng, J.K., Zheng, C., Taipale, A., Zhang, Y., Takara, K., Bruce, J.E.: Quantitative interactome analysis reveals a chemoresistant edgotype. *Nat. Commun.* **6**, 7928 (2015)
30. Ihling, C., Falvo, F., Kratochvil, I., Sinz, A., Schäfer, M.: Dissociation behavior of a bifunctional tempo-active ester reagent for peptide structure analysis by free radical initiated peptide sequencing (FRIPS) mass spectrometry. *J. Mass Spectrom.* **50**, 396–406 (2015)
31. Hodyss, R., Cox, H.A., Beauchamp, J.L.: Bioconjugates for tunable peptide fragmentation: free radical initiated peptide sequencing (FRIPS). *J. Am. Chem. Soc.* **127**, 12436–12437 (2005)
32. Gao, J., Thomas, D.A., Sohn, C.H., Beauchamp, J.L.: Biomimetic reagents for the selective free radical and acid–base chemistry of glycans: application to glycan structure determination by mass spectrometry. *J. Am. Chem. Soc.* **135**, 10684–10692 (2013)
33. Thomas, D.A., Sohn, C.H., Gao, J., Beauchamp, J.L.: Hydrogen bonding constrains free radical reaction dynamics at serine and threonine residues in peptides. *J. Phys. Chem. A* **118**, 8380–8392 (2014)
34. Marshall, D.L., Hansen, C.S., Trevitt, A.J., Oh, H.B., Blanksby, S.J.: Photodissociation of TEMPO-modified peptides: new approaches to radical-directed dissociation of biomolecules. *Phys. Chem. Chem. Phys.* **16**, 4871–4879 (2014)
35. Oh, H.B., Moon, B.: Radical-driven peptide backbone dissociation tandem mass spectrometry. *Mass Spectrom. Rev.* **34**, 116–132 (2015)
36. Lee, J., Park, H., Kwon, H., Kwon, G., Jeon, A., Kim, H.I., Sung, B.J., Moon, B., Oh, H.B.: One-step peptide backbone dissociations in negative-ion free radical initiated peptide sequencing mass spectrometry. *Anal. Chem.* **85**, 7044–7051 (2013)
37. Lowe, T.A., Paine, M.R., Marshall, D.L., Hick, L.A., Boge, J.A., Barker, P.J., Blanksby, S.J.: Structural identification of hindered amine light stabilisers in coil coatings using electrospray ionisation tandem mass spectrometry. *J. Mass Spectrom.* **45**, 486–495 (2010)
38. Marshall, D.L., Gryn'ova, G., Coote, M.L., Barker, P.J., Blanksby, S.J.: Experimental evidence for competitive N–O and O–C bond homolysis in gas-phase alkoxyamines. *Int. J. Mass Spectrom.* **378**, 38–47 (2015)
39. Jeon, A., Lee, J.H., Kwon, H.S., Park, H.S., Moon, B.J., Oh, H.B.: Charge-directed peptide backbone dissociations of o-TEMPO-Bz-C(O)-peptides. *Mass Spectrom. Lett* **4**, 71–74 (2013)
40. Gryn'ova, G., Marshall, D.L., Blanksby, S.J., Coote, M.L.: Switching radical stability by pH-induced orbital conversion. *Nat. Chem.* **5**, 47–481 (2013)
41. Gotze, M., Pettelkau, J., Fritzsche, R., Ihling, C.H., Schäfer, M., Sinz, A.: Automated assignment of MS/MS cleavable cross-links in protein 3D-structure analysis. *J. Am. Soc. Mass Spectrom.* **26**, 83–97 (2015)
42. Kalkhof, S., Sinz, A.: Chances and pitfalls of chemical cross-linking with amine-reactive N-hydroxysuccinimide esters. *Anal. Bioanal. Chem.* **392**, 305–312 (2008)
43. Sonsmann, G., Romer, A., Schomburg, D.: Investigation of the influence of charge derivatization on the fragmentation of multiply protonated peptides. *J. Am. Soc. Mass Spectrom.* **13**, 47–58 (2002)
44. Hao, P., Adav, S.S., Gallart-Palau, X., Sze, S.K.: Recent advances in mass spectrometric analysis of protein deamidation. *Mass Spectrom. Rev.* (2016). doi:10.1002/mas.21491